Cerebral Cortex, 2021;00: 1–12

https://doi.org/10.1093/cercor/bhab380
Original Article

ORIGINAL ARTICLE

Resting-State fMRI Functional Connectivity Strength Predicts Local Activity Change in the Dorsal Cingulate Cortex: A Multi-Target Focused rTMS Study

Zi-Jian Feng[1,2,3], Xin-Ping Deng[1,2,3], Na Zhao[1,2,3], Jing Jin[1,2,3], Juan Yue[1,2,3], Yun-Song Hu[1,2,3], Ying Jing[1,2,3], Hong-Xiao Wang[1,2,3], Thomas R. Knösche[4], Yu-Feng Zang[1,2,3] and Jue Wang[5]

[1]Center for Cognition and Brain Disorders, The Affiliated Hospital of Hangzhou Normal University, Hangzhou 310015, China, [2]Institute of Psychological Sciences, Hangzhou Normal University, Hangzhou 311121, China, [3]Zhejiang Key Laboratory for Research in Assessment of Cognitive Impairments, Hangzhou 310015, China, [4]Max Planck Institute for Human Cognitive and Brain Sciences, Leipzig 04103, Germany and [5]Institute of sports medicine and health, Chengdu Sport University, Chengdu 610041, China

Address correspondence to Jue Wang, Institute of sports medicine and health, Chengdu Sport University, No. 2, Tiyuan Rd, Wuhou District, Chengdu, 610041, China. Email: juefirst@cdsu.edu.cn and Yu-Feng Zang, Institutes of Psychological Sciences, Hangzhou Normal University, No. 2318, Yuhangtang Rd, Yuhang District, Hangzhou, 311121, China. Email: zangyf@hznu.edu.cn

Abstract

Previous resting state functional magnetic resonance imaging (RS-fMRI) studies suggested that repetitive transcranial magnetic stimulation (rTMS) can modulate local activity in distant areas via functional connectivity (FC). A brain region has more than one connection with the superficial cortical areas. The current study proposed a multi-target focused rTMS protocol for indirectly stimulating a deep region, and to investigate 1) whether FC strength between stimulation targets (right middle frontal gyrus [rMFG] and right inferior parietal lobule [rIPL]) and effective region (dorsal anterior cingulate cortex [dACC]) can predict local activity changes of dACC and 2) whether multiple stimulation targets can focus on the dACC via FC. A total of 24 healthy participants received rTMS with two stimulation targets, both showing strong FC with the dACC. There were four rTMS conditions (>1 week apart, 10 Hz, 1800 pulses for each): rMFG-target, rIPL-target, Double-targets (900 pulses for each target), and Sham. The results failed to validate the multi-target focused rTMS hypothesis. But rMFG-target significantly decreased the local activity in the dACC. In addition, stronger dACC-rMFG FC was associated with a greater local activity change in the dACC. Future studies should use stronger FC to focus stimulation effects on the deep region.

Key words: functional connectivity, local activity, multi-target focused, RS-fMRI, rTMS

Introduction

Repetitive transcranial magnetic stimulation (rTMS) is a non-invasive brain stimulation technique that has gained official approval for therapy of some brain disorders, including depression (Cash et al. 2020), migraines (Shehata et al. 2016), and obsessive–compulsive disorder (Lee et al. 2017). Although figure-8 coil transcranial magnetic stimulation (TMS) provides a relatively focal magnetic field, the exact location of the stimulation target

in routine rTMS treatment is largely unknown. For example, the most popular "5-cm" localization method is claimed to target the dorsolateral prefrontal cortex (DLPFC). However, it is highly variable in spatial distance between individuals, ranging from the premotor cortex to the frontal eye fields (Herwig et al. 2001; Herbsman et al. 2009; Ahdab et al. 2010; Padmanabhan et al. 2019). This variation is likely to be the primary cause of the substantial variability in rTMS efficacy (Cash et al. 2020).

It has been proposed that the functional connectivity (FC) of resting-state functional magnetic resonance imaging (RS-fMRI) could be useful for accurate guidance of the location of rTMS targets. The subgenual anterior cingulate cortex (sgACC) is a key brain region associated with depression (Drevets et al. 2008). Many RS-fMRI studies have demonstrated an anticorrelation (i.e., negative FC) between the sgACC and DLPFC, and that a stronger negative FC between the sgACC and stimulation target in the DLPFC predicts better efficacy of rTMS treatment of depression (Fox et al. 2012; Li et al. 2014; Weigand et al. 2018; Cash et al. 2019; Siddiqi et al. 2019; Jing et al. 2020). These findings indicate that rTMS over the DLPFC stimulation target indirectly affects the sgACC via FC. As a counterpart of the "stimulation target" on the superficial cortex, we refer to this deep region as the "effective region" hereafter, as in our previous study (Jing et al. 2020).

Several RS-fMRI studies reported that FC strength was modulated by FC-guided rTMS (Wang et al. 2014; Williams et al. 2018; Freedberg et al. 2019; Cole et al. 2020; Hendrikse et al. 2020). However, RS-fMRI FC reflects the relationship between two brain regions, and changes in FC alone cannot indicate which specific brain region is changed. In addition to FC, RS-fMRI can also measure local activity (e.g., regional homogeneity [ReHo]) (Zang et al. 2004), a metric of local synchronization and the percent amplitude of fluctuation (PerAF) (Jia et al. 2020), a more reliable derivative of the amplitude of low-frequency fluctuation (ALFF) (Zang et al. 2007) of each single voxel. These two indices can directly measure whether the local activity of the effective region is modulated by rTMS (Ruan et al. 2019; Wang et al. 2020). In addition, previous studies have found that rTMS alters the local activity of remote brain regions (Xue et al. 2017; Grohn et al. 2019; Guo et al. 2019; Ruan et al. 2019; Wang et al. 2020; Yin et al. 2020; Zheng et al. 2020; Yuan et al. 2021), but none of these studies were FC-guided. Thus, there remains a dearth of knowledge about whether the effects of rTMS on the stimulation target can alter local activity in the effective region, whether rTMS can cause changes in FC between the stimulation target and the effective region, and whether pre-rTMS FC strength predicts such local activity changes.

Any effective region has more than one connection with the superficial cortical areas. However, previous FC-guided rTMS studies have only used "one-to-one" stimulation, in which one effective region corresponds to only one stimulation target in the superficial cortex (Wang et al. 2014; Wang and Voss 2015; Freedberg et al. 2019; Hendrikse et al. 2020). A recent review proposed that the TMS target definition can also be based on symptom/function-specific brain networks (Cash et al. 2020). The dorsal anterior cingulate cortex (dACC) is part of the cingulo-frontal–parietal (CFP) cognitive-attention network involved in attention, cognition, executive function, and response inhibition (Bush 2011). Our previous studies (Zang et al. 2007; Yan et al. 2009; Wang et al. 2013; Wang et al. 2015) focused on the attentional function of the dACC, which is one of the most consistently reported abnormal brain regions in attention deficit hyperactivity disorder (Lei et al. 2015; Norman et al. 2016). Moreover, the dACC has been found to have a strong connection with other cognitive-attention network-related regions, including the DLPFC and parietal cortex in monkey studies (Morecraft and Tanji 2009; Rolls 2009) and human studies (Bush 2011). Both the frontal and parietal cortices of the CFP are good candidate TMS targets because of their superficial location. Therefore, we proposed the multi-target focused rTMS (MTF-rTMS) protocol for indirectly stimulating the dACC. We hypothesized that multiple stimulation targets would exhibit focused effects on the same effective region (i.e., the dACC). In addition, we hypothesized that the focused effect would be similar to that of a single target if the total pulses were the same.

The present study aimed to investigate two main issues: 1) whether the FC strength of stimulation targets with the dACC could predict the local activity change in dACC; and 2) whether MTF-rTMS can modulate local activity in the effective region (i.e., dACC) via FC.

Table 1 Exclusion criteria

	N
Failed to complete the cognitive task	3
Did not meet the criteria for defining the TMS target	3
Extreme value	2
Large head motion	1

Materials and Methods

The current study was approved by the Ethics Committee of the Center for Cognition and Brain Disorders (CCBD) at Hangzhou Normal University (HZNU). All participants provided written informed consent before the experiment, in accordance with the Declaration of Helsinki.

Participants

In total, 33 healthy participants (19–29 years old, 22.6 ± 2.5 years old, 19 females) were recruited. None of the participants had any history of neurological or psychiatric disorders or head injury. In total, nine participants were excluded (Table 1). Three participants failed to complete the cognitive task, three did not meet the criteria for defining the TMS target (see sections 2.6.2 and 2.6.3 for details), two exhibited extreme values (see section 2.8.2 for details), and one showed excessive head motion (exceeding 2 mm in translation and 2° in rotation in any direction for any session). Thus, 24 participants (19–29 years old, 22.6 ± 2.6 years old, 12 females) were included in the statistical analysis. The study was registered at ClinicalTrials.gov (NCT03515408).

Overall Protocol

A flowchart of the experiment is shown in Figure 1. The current study had a within-subject design. Testing was performed on four separate days (at least 1 week apart) corresponding to four counterbalanced conditions of rTMS intervention. On each day, the procedure included a pre-rTMS RS-fMRI scanning, a measurement of the resting motor threshold (RMT), an rTMS intervention, and an immediate post-rTMS RS-fMRI scanning. For MRI scanning on the first day (Visit 1), 3D-T1 MRI and task fMRI were obtained for localization and navigation purposes. The peak voxel of task fMRI activation for each participant in

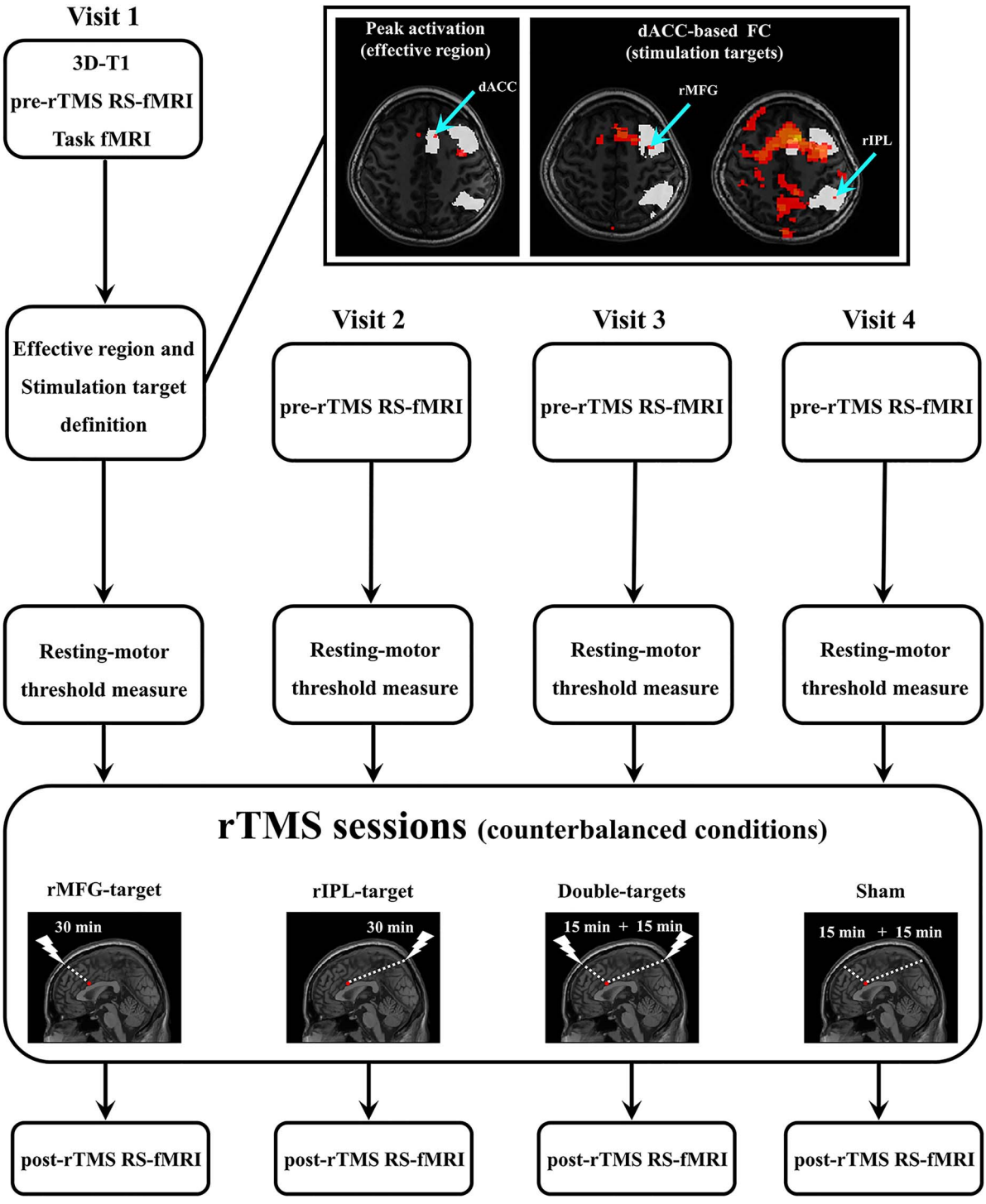

Figure 1. The schematic protocol of Experiment. rTMS, repetitive transcranial magnetic stimulation; fMRI, functional magnetic resonance imaging; RS-fMRI, resting-state fMRI; FC, functional connectivity; dACC, dorsal anterior cingulate cortex; rMFG, right middle frontal gyrus; rIPL, right inferior parietal lobule; rMFG-target, rMFG single-target condition; rIPL-target, rIPL single-target condition; Double-targets, double-targets condition.

a dACC mask (see section "2.5. Masks for the effective region and stimulation targets") was defined as the seed for the RS-fMRI FC analysis. Individualized FC peaks in the right middle frontal gyrus (rMFG) and right inferior parietal lobule (rIPL) were determined as the stimulation targets.

RS-fMRI and Task fMRI Design

During RS-fMRI scanning, participants were instructed to close their eyes, relax, remain motionless, not think of anything in particular, and not fall asleep. RS-fMRI scanning lasted 8 min.

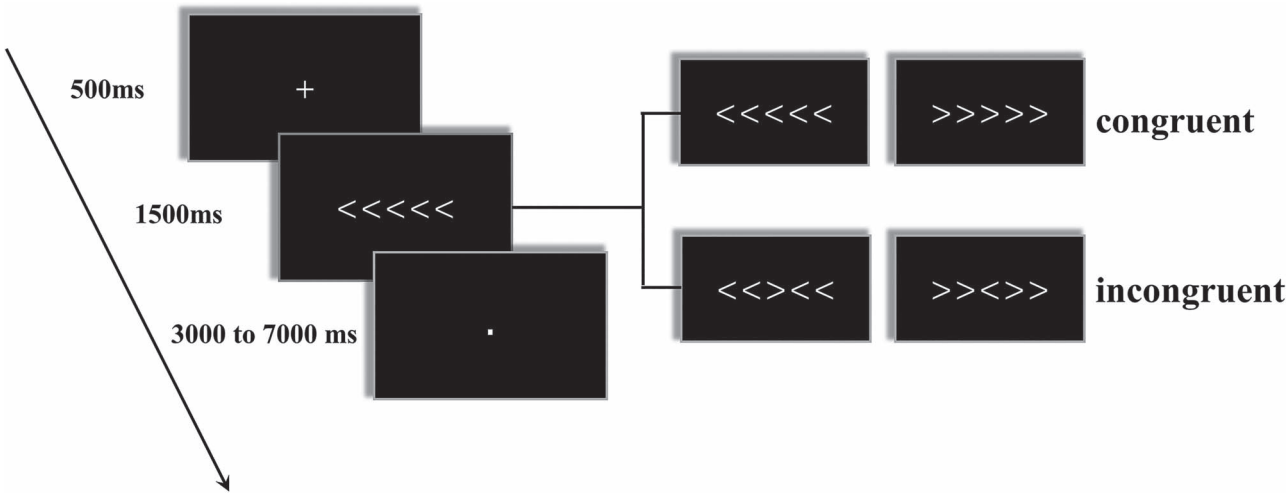

Figure 2. Eriksen flanker, an event related design task, during an 18.8-min fMRI scan.

For the task fMRI, the Eriksen flanker task (EFT) (Eriksen and Eriksen 1974) was employed (Fig. 2). Participants practiced the task outside the scanner shortly before scanning. The EFT was programmed in E-prime 2.0 (Psychology Software Tools, Inc.). Participants were instructed to press the left or right button with their right index finger as soon as possible to respond to the direction of the central arrow (< or >) in a row of five arrows. In a total of 160 sessions (18.8 min), there were four stimuli with the same probability of occurrence, two of which were congruent conditions (<<<<< or >>>>>) and two of which were incongruent conditions (<<><< or >><>>). In each trial, a fixation cross (+) was presented for 500 ms, then the arrows appeared for 1500 ms, followed by a dot in a pseudorandom order for 3000–7000 ms.

MRI Data Acquisition

All MRI data were obtained on a 3 T scanner (MR-750, GE Medical Systems, Milwaukee, WI) at the Center for Cognition and Brain Disorders of Hangzhou Normal University. Comfortable straps and foam pads were used to minimize head motion. High-resolution T1-weighted anatomical images were acquired using a 3D spoiled gradient echo sequence with the following parameters: sagittal slices; slice number = 176; matrix size = 256 × 256; field of view (FOV) = 256 × 256 mm^2; repetition time/echo time (TR/TE) = 8.1/3.1 ms; fractional isotropy (FA) = 8°; thickness/gap = 1/0 mm (isotropic voxel size = 1 mm × 1 mm × 1 mm). fMRI images using an echo-planar imaging (EPI) sequence were acquired with the following parameters: TE = 30 ms; FA = 90°; TR = 2000 ms; 43 slices with interleaved acquisition; thickness/gap = 3.2/0 mm; FOV = 220 × 220 mm^2; matrix = 64 × 64; and voxel size = 3.44 mm × 3.44 mm × 3.2 mm.

Masks for the Effective Region and Stimulation Targets

To define the individual effective region and stimulation targets, three masks were constructed. The effective region was defined in a dACC-Mask (Fig. 3) which was constructed by combining the delineation reported by Bush et al. (2000) and the automated anatomical labeling (AAL) template (Tzourio-Mazoyer et al. 2002), as in our previous study (Yan et al. 2009; Wang et al. 2013).

The parietal and frontal stimulation targets were defined in an rIPL-Mask and rMFG-Mask, respectively. The rIPL-Mask was generated from the AAL template (Tzourio-Mazoyer et al. 2002). Because the rMFG region is very large in the AAL template, the rMFG-Mask was generated from the Harvard-Oxford cortical structural atlases with a gray matter probability threshold of 25% (http://fsl.fmrib.ox.ac.uk/fsl/fslwiki/Atlases). We chose these two stimulation targets on the basis of the following considerations:

1) The frontal lobe, parietal lobe, and dACC serve as vital nodes of the cognitive-attention network (Bush 2011). Our previous studies revealed that the dACC exhibited significant resting-state FC with widespread brain regions including the rMFG and the rIPL (Yan et al. 2009; Wang et al. 2015). To validate the dACC seed-based resting-state FC pattern, we performed a preliminary study (see Supplementary Material, SM1) and found that each participant's dACC exhibited FC with these two superficial regions (Fig. S1).

2) The position of these two superficial regions is convenient for rTMS intervention.

MRI Data Processing for Navigation Purposes

Data Processing for Structural MRI

The T1 image was re-oriented manually, then segmented into gray matter, white matter, and cerebrospinal fluid using SPM12 (http://www.fil.ion.ucl.ac.uk/spm/software/spm12/). The spatial normalization parameters were used to transform back and forth between standard space and original space in the subsequent fMRI data analyses.

Task fMRI Activation and Localization of the Effective Region

Preprocessing included the following procedures: 1) slice timing correction; 2) head motion correction; 3) co-registration of EPI images and the T1 image (See more details in SM2 in Supplementary Material); and 4) spatial smoothing with a Gaussian kernel (full-width half-maximum [FWHM] = 6 mm). Immediately after scanning on the first day, the individual activation map of both the incongruent condition (hereafter referred to as I condition) and incongruent minus congruent condition (hereafter referred to as I-C condition) were generated in the original space

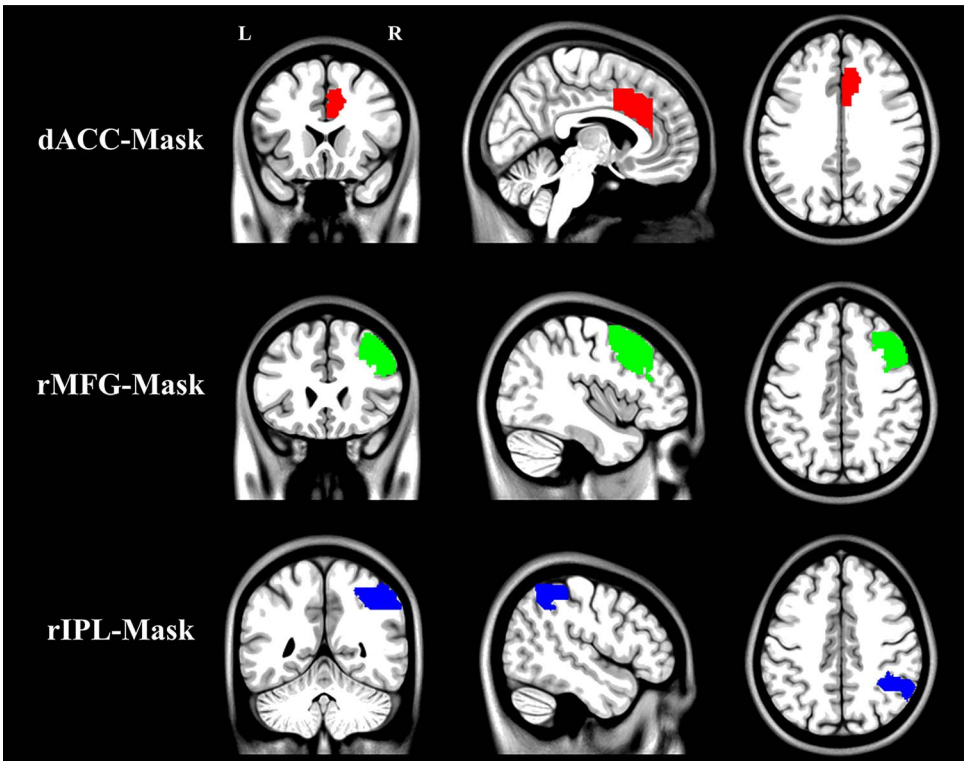

Figure 3. The effective region (dACC-Mask) and stimulation targets (rMFG-Mask and rIPL-Mask). dACC, dorsal anterior cingulate cortex; rMFG, right middle frontal gyrus; rIPL, right inferior parietal lobule; L: left; R: right.

of each participant. To locate the individual peak activation voxel in the dACC, the dACC-Mask was warped inversely from Montreal Neurological Institute (MNI) space to the original space for each participant. Then, the individual peak activation voxel of the I-C condition was defined as the effective region for each participant. If there was no significant activation of I-C at a threshold of $P < 0.05$, the I condition was used to define the individual effective region. Finally, the effective region was obtained by employing the I-C condition in seven participants and by employing the I condition in 17 participants. The exact location of the group-level peak voxel in the I-C condition (x = 9, y = 9, z = 45, seven participants) was very close to that in the I condition (x = 9, y = 12, z = 45, 17 participants). The MNI coordinates of each participant's effective region are shown in Table 2. As mentioned above, one participant was excluded because they showed no significant activation ($P > 0.05$) in either the I-C or I-condition.

Localization of Individual Stimulation Targets by dACC FC

The preprocessing procedure for RS-fMRI included the following steps: 1) removal of the first 10 volumes; 2) slice timing correction; 3) head motion correction; 4) co-registration of all the EPI images to the T1 image; 5) regressing out the signals of white matter, cerebrospinal fluid and head motion parameters with the Friston-24 model; 6) removal of linear trends; and 7) temporal band-pass filtering (0.01–0.08 Hz).

For individual RS-fMRI FC analysis of the dACC, a spherical seed region of interest (ROI) (4 mm radius) was centered at the activation peak voxel in the dACC-Mask of each participant in the original space. The mean RS-fMRI time course within the seed ROI was extracted. Spatial smoothing (FWHM = 6 mm) was then performed on the preprocessed data. Voxel-wise FC using Pearson's correlation was then calculated for each participant in the original space.

The voxel with the strongest FC was selected within the rMFG-Mask and rIPL-Mask separately for each participant in the original space. The following *ad hoc* criteria were used to define the stimulation target: 1) located in the superficial cortex within a depth of 4 cm beneath the scalp; and 2) FC (i.e., *r*) value greater than 0.1. Two participants were excluded because the FC (i.e., *r*) value was less than 0.1. Finally, we double-checked and found that the targets of eight participants were localized outside the mask (by a distance of one voxel). All of the other 16 participants' targets were within the mask. The MNI coordinates of the individual's stimulation targets are shown in Tables 3 and 4. We plotted all of the individual MNI coordinates of the stimulation targets and the deep effective region (Fig. 4).

Stimulation Protocol

rTMS (Magstim Super Rapid^2, Magstim Co., Whitland, United Kingdom) was delivered using a 70-mm biphasic figure-8 coil with a special air-cooling system. Frameless stereotaxic neuronavigation (Brainsight, Rogue Research, Montreal, Canada) was used to track the coil and head positions. Individual RMT was measured prior to rTMS for each visit. RMT was determined by a single pulse stimulation by orienting the coil 45° toward the contralateral forehead to evoke the "hotspot" motor response (>50 μV) of the right first dorsal interosseous (FDI) muscle with the lowest intensity, in at least five of 10 consecutive trials (Rossini et al. 2015).

Each participant received four rTMS sessions on four different days: the rMFG single-target condition (rMFG-target), rIPL

Table 2 Individualized peak activation coordinates of task fMRI within the dACC-Mask

Subject ID	MNI Coordinate			T value	P value (uncorrected)
	X	Y	Z		
Sub001	11	12	35	2.74	<0.01
Sub002	14	13	41	2.09	<0.05
Sub003	2	23	31	2.41	<0.05
Sub004	9	30	39	2.11	<0.05
Sub005	9	8	34	4.24	<0.0001
Sub006	10	23	40	7.63	<0.0001
Sub007	9	23	33	2.68	<0.01
Sub008	11	22	35	3.98	<0.0001
Sub009	11	13	35	2.35	<0.05
Sub010	11	13	46	5.86	<0.0001
Sub011	10	23	25	6.93	<0.0001
Sub012	11	18	35	2.18	<0.05
Sub013	10	17	39	6.41	<0.0001
Sub014	13	19	31	2.52	<0.05
Sub015	10	29	38	2.84	<0.01
Sub016	10	12	46	2.29	<0.05
Sub017	4	26	35	2.71	<0.01
Sub018	11	8	32	2.48	<0.05
Sub019	11	13	47	8.86	<0.0001
Sub020	8	28	26	3.47	<0.001
Sub021	9	15	45	6.89	<0.0001
Sub022	6	20	42	2.84	<0.01
Sub023	10	20	48	7.94	<0.0001
Sub024	12	16	44	8.42	<0.0001
Mean ± SD	9.7 ± 2.6	18.5 ± 6.4	37.6 ± 6.4		

dACC, dorsal anterior cingulate cortex; MNI, Montreal Neurological Institute. T, the *t* value of individualized peak activation voxel; P, corresponding *p* value of the individualized peak activation voxel.

Table 3 Individualized rMFG target coordinates and corresponding r value of FC with the dACC seed

Subject ID	MNI coordinate			r value
	X	Y	Z	
Sub001	48	0	54	0.500
Sub002	37	0	56	0.608
Sub003	45	32	25	0.180
Sub004	34	23	47	0.571
Sub005	33	27	47	0.324
Sub006	39	9	49	0.453
Sub007	51	34	35	0.206
Sub008	42	10	55	0.501
Sub009	39	3	57	0.652
Sub010	42	8	42	0.456
Sub011	44	1	56	0.485
Sub012	41	0	56	0.518
Sub013	40	5	55	0.310
Sub014	29	5	56	0.595
Sub015	37	33	41	0.617
Sub016	31	27	38	0.648
Sub017	38	2	47	0.602
Sub018	30	9	58	0.414
Sub019	35	4	43	0.759
Sub020	37	10	62	0.192
Sub021	46	0	54	0.669
Sub022	30	32	34	0.539
Sub023	45	13	35	0.505
Sub024	36	30	43	0.414
Mean ± SD	38.7 ± 6.0	13.2 ± 12.6	47.7 ± 9.6	0.488

rMFG, right middle frontal gyrus; dACC, dorsal anterior cingulate cortex; FC, functional connectivity; MNI, Montreal Neurological Institute.

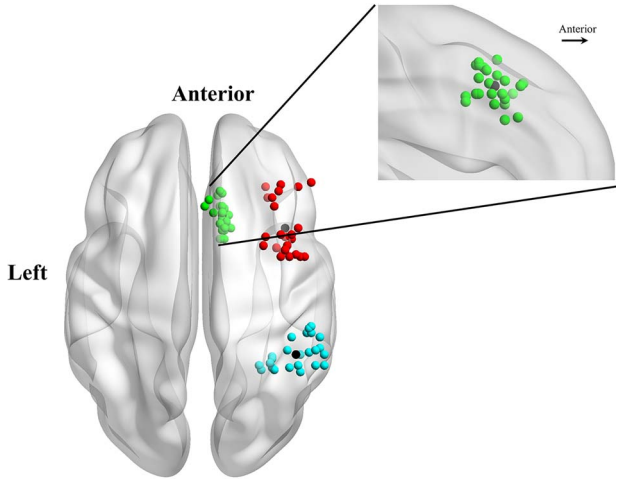

Figure 4. The spatial distribution of the individual effective region (green dots) and the individual stimulation targets (rMFG with red dots and rIPL with blue dots) for all participants. The black dots indicate the mean coordinates. rMFG, right middle frontal gyrus; rIPL, right inferior parietal lobule.

single-target condition (rIPL-target), double-targets condition (Double-targets), and sham condition (Sham). For the rMFG-target and rIPL-target conditions, rTMS pulses were delivered to the stimulation target in the rMFG and rIPL separately with the following parameters: 60 trains (3 s duration at 10 Hz with an inter-train interval of 27 s), 1800 pulses and 30 min in total. For the Double-targets condition, 900 pulses were delivered to the rMFG and the rIPL targets separately, with the order of the rMFG target and rIPL target counterbalanced across participants. The other parameters were the same as those in the single-target condition. The protocol in the Sham condition was the same as that in the Double-targets condition, except that the coil was positioned with the lateral edge of one wing touching the scalp at 90° (Pascual-Leone et al. 1996).

RS-fMRI Data Analysis for Detection of rTMS Effects

RS-fMRI Data Preprocessing

The RS-fMRI data preprocessing for detection of the rTMS effects included the following steps: 1) removal of the first 10 volumes; 2) slice timing correction; 3) head motion correction 4) spatial normalization to standard MNI space using the EPI template; 5) regressing out the signals of white matter, cerebrospinal fluid, and head motion (Friston 24 model); 6) removal of linear trends; 7) temporal band-pass filtering (0.01–0.08 Hz); and 8) spatial smoothing (FWHM = 6 mm).

Calculation of Local Brain Activity

Percent amplitude of fluctuation (PerAF). ALFF (Zang et al. 2007) is a widely used metric to measure the local activity of RS-fMRI. The PerAF has been reported to exhibit similar test–retest (i.e., intra-scanner) reliability to ALFF, but higher inter-scanner reliability (Zhao et al. 2018). We used the RESTplus (V1.2, http://restfmri.net) toolkit (Jia et al. 2019) to calculate PerAF. For standardization purposes, we normalized PerAF to mPerAF by dividing each voxel by the global mean PerAF. Then, the mPerAF change (post-rTMS minus pre-rTMS) was calculated.

Table 4 Individualized rIPL target coordinates and corresponding r value of FC with the dACC seed

Subject ID	MNI coordinate			r value
	X	Y	Z	
Sub001	32	−49	55	0.497
Sub002	57	−45	57	0.224
Sub003	57	−50	37	0.293
Sub004	55	−42	53	0.660
Sub005	53	−43	54	0.353
Sub006	50	−44	47	0.252
Sub007	33	−46	48	0.284
Sub008	51	−32	55	0.321
Sub009	33	−47	50	0.160
Sub010	50	−33	55	0.262
Sub011	51	−35	54	0.254
Sub012	45	−50	55	0.252
Sub013	42	−37	52	0.309
Sub014	33	−51	51	0.591
Sub015	46	−53	54	0.523
Sub016	34	−52	52	0.543
Sub017	49	−35	49	0.612
Sub018	27	−50	52	0.330
Sub019	40	−43	45	0.477
Sub020	28	−52	51	0.427
Sub021	46	−45	41	0.381
Sub022	53	−50	51	0.560
Sub023	41	−51	46	0.530
Sub024	55	−37	48	0.484
Mean ± SD	44.2 ± 9.6	−44.67 ± 6.6	50.5 ± 4.8	0.399

rIPL, right inferior parietal lobule; dACC, dorsal anterior cingulate cortex; FC, functional connectivity; MNI, Montreal Neurological Institute.

Regional homogeneity (ReHo). The Kendall coefficient of concordance (KCC) of the given voxel with its 27 neighboring voxels was calculated as the ReHo of the given voxel (Zang et al. 2004). The ReHo value of each voxel was divided by the whole-brain mean ReHo value, and mReHo was obtained. Because smoothing before the mReHo calculation increases the regional homogeneity among voxels, spatial smoothing (FWHM = 6 mm) was performed on the mReHo map. The mReHo change (post-rTMS minus pre-rTMS) was then calculated.

Individual spherical ROIs (radius = 4 mm) were centered at the rMFG-target, rIPL-target, and the effective region (i.e., dACC), separately. Within each ROI, the mean value of the local activity change (i.e., post-rTMS minus pre-rTMS) was extracted separately for mPerAF and mReHo. Two participants were excluded because their local activity change (mReHo and mPerAF change) in the dACC exceeded three standard deviations.

Calculation of FC

The mean time course of each ROI (individualized dACC, rMFG, and rIPL) was extracted from the preprocessed RS-fMRI data. ROI-wise FC was then calculated between the effective region (i.e., dACC) and stimulation targets (i.e., rMFG and rIPL). The *r*-value was transformed to a *z*-value using Fisher's *z*-transformation.

Statistical Analyses

FC Strength Predicts the Local Activity Change in the dACC

To investigate the rTMS effect on the local activity in the dACC, we conducted paired *t*-tests on the local activity (i.e., post-rTMS versus pre-rTMS for both mPerAF and mReHo) in the effective region (i.e., dACC) in each of the four rTMS conditions (rMFG-target, rIPL-target, Double-targets, and Sham). Furthermore, we performed Pearson's correlation analyses between the strength of FCs (i.e., dACC-rMFG and dACC-rIPL) and the local activity change of the dACC in each of the four conditions to explore whether the FC strength predicted the local activity change.

In addition, to explore the rTMS effect on the local activity in the stimulation targets, paired *t*-tests were performed on the local activity (i.e., post-rTMS versus pre-rTMS for the mPerAF and mReHo in the rMFG and rIPL, respectively) in each of the four rTMS conditions (rMFG-target, rIPL-target, Double-targets, and Sham).

Table 5 The rTMS induced mReHo changes (post-rTMS vs. pre-rTMS) in the stimulation targets (rMFG, rIPL) and the effective region (dACC)

ROI	mReHo (Mean ± SD)		T	P
	Pre-TMS	Post-TMS		
Double-targets				
dACC	1.00 ± 0.21	1.01 ± 0.18	0.106	0.917
rMFG	1.18 ± 0.27	1.18 ± 0.22	-0.010	0.992
rIPL	1.31 ± 0.36	1.32 ± 0.37	0.276	0.785
rMFG-target				
dACC	1.09 ± 0.21	1.03 ± 0.20	-3.389	0.003**
rMFG	1.16 ± 0.26	1.21 ± 0.25	1.260	0.220
rIPL	1.30 ± 0.32	1.36 ± 0.35	2.133	0.044*
rIPL-target				
dACC	1.02 ± 0.22	1.01 ± 0.16	-0.400	0.693
rMFG	1.21 ± 0.28	1.20 ± 0.27	-0.301	0.766
rIPL	1.34 ± 0.30	1.30 ± 0.33	-0.809	0.427
Sham				
dACC	1.04 ± 0.18	1.01 ± 0.19	-1.084	0.289
rMFG	1.26 ± 0.21	1.21 ± 0.28	-1.720	0.099
rIPL	1.27 ± 0.30	1.32 ± 0.32	1.510	0.145

mReHo, mean regional homogeneity; pre-rTMS, before rTMS session; post-rTMS, after rTMS session; dACC, dorsal anterior cingulate cortex; rMFG, right middle frontal gyrus; rIPL, right inferior parietal lobule; rMFG-target, rMFG single-target condition; rIPL-target, rIPL single-target condition; Double-targets, double-targets condition; *$P < 0.05$ uncorrected; **, Still significant after Bonferroni correction of 0.05/12 = 0.004.

Testing whether MTF-rTMS (i.e., Double-Targets) Differs from Single-Target rTMS

For the local activity change (i.e., post-rTMS minus pre-rTMS for both mPerAF and mReHo), we conducted a one-way repeated-measures analysis of variance (ANOVA) (SPSS v25.0, SPSS Inc., Chicago, IL, USA) among the four rTMS conditions (rMFG-target, rIPL-target, Double-targets, and Sham). In addition, for the FC change, a one-way repeated-measures ANOVA was performed among the four rTMS conditions. It should be noted that for the Double-targets and Sham conditions, we calculated both the dACC-rMFG and dACC-rIPL FC changes. Therefore, there were six levels in the ANOVA for FC change.

Results

Pre-rTMS dACC FC Strength Predicted Local Activity Change in the dACC

Paired *t*-tests revealed that the rMFG-target intervention significantly decreased mReHo in the dACC ($t = -3.389$, $P = 0.003$, Bonferroni correction, i.e., 0.05/12 = 0.004; Fig. 5a and Table 5). Moreover, the rMFG-target intervention showed a trend toward

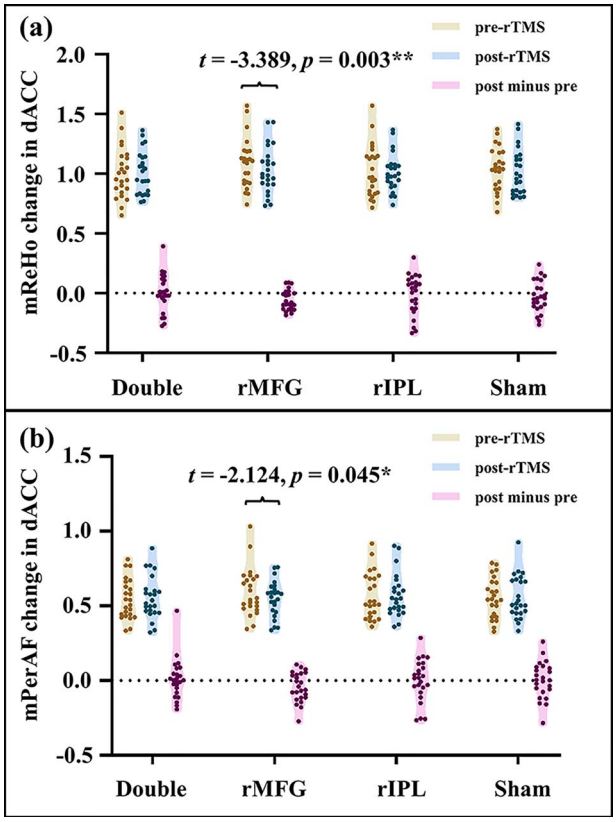

Figure 5. The local activity in the effective region (dACC). (a) Paired *t*-tests (post- vs. pre-rTMS) showed significantly decreased mReHo in the dACC only when stimulated the rMFG-target. (b) Paired *t*-tests (post- vs. pre-rTMS) showed a trend of decreased mPerAF in the dACC when stimulated the rMFG-target. mReHo, mean regional homogeneity; mPerAF, mean percent amplitude of fluctuation; dACC, dorsal anterior cingulate cortex; rMFG, right middle frontal gyrus; rIPL, right inferior parietal lobule; rMFG-target, rMFG single-target condition; rIPL-target, rIPL single-target condition; Double-targets, double-targets condition; *$P < 0.05$ uncorrected; **, still significant after Bonferroni correction of $0.05/12 = 0.004$.

decreased mPerAF in the dACC ($t = -2.124$, $P = 0.045$, uncorrected; Fig. 5b and Table 6). Correlation analyses revealed a significant negative correlation between the pre-rTMS FC of dACC-rMFG and the mReHo change of the dACC ($r = -0.549$, $P = 0.005$, surviving Bonferroni correction, i.e., $0.05/6 = 0.008$; Fig. 6a) as well as the mPerAF change in the dACC ($r = -0.452$, $P = 0.026$, uncorrected; Fig. 6b) in the rMFG-target condition, suggesting that the pre-rTMS FC of the dACC-rMFG predicted local activity change in the dACC. Stronger dACC-rMFG FC was associated with a greater local activity decrease in the dACC.

Paired *t*-tests revealed no significant differences in other comparisons of local activity (Tables 4 and 5). For the rest of the correlations between FC strength before each rTMS condition and the local activity change in the effective region of that condition, please see the Supplementary Material (Figs S2 and S3).

The Difference between MTF-rTMS (I.E., Double-Targets) and Single-Target rTMS

For the local activity change (i.e., post-rTMS minus pre-rTMS for both mPerAF and mReHo), we did not find significant difference among the four rTMS conditions (rMFG-target, rIPL-target, Double-targets, and Sham) in any ROI (the effective region of dACC, and stimulation targets of rMFG and rIPL) for either mPerAF or mReHo ($Fs = 0.17–1.72$, $Ps = 0.17–0.92$). The FC change showed no significant difference among the four rTMS conditions (six levels) ($F = 0.602$, $P = 0.612$).

Table 6 The rTMS induced mPerAF changes (post-rTMS vs. pre-rTMS) in the stimulation targets (rMFG, rIPL) and the effective region (dACC)

ROI	mPerAF (Mean ± SD)		T	P
	Pre-TMS	Post-TMS		
Double-targets				
dACC	0.55 ± 0.14	0.54 ± 0.13	0.390	0.700
rMFG	0.74 ± 0.34	0.75 ± 0.27	-0.349	0.730
rIPL	0.93 ± 0.51	0.91 ± 0.52	0.482	0.635
rMFG-target				
dACC	0.55 ± 0.12	0.59 ± 0.16	-2.124	0.045*
rMFG	0.73 ± 0.23	0.73 ± 0.32	0.035	0.973
rIPL	0.89 ± 0.46	0.90 ± 0.54	-0.053	0.958
rIPL-target				
dACC	0.57 ± 0.14	0.57 ± 0.15	0.018	0.986
rMFG	0.73 ± 0.23	0.76 ± 0.29	-1.035	0.311
rIPL	0.91 ± 0.48	0.91 ± 0.50	-0.027	0.978
Sham				
dACC	0.56 ± 0.14	0.56 ± 0.13	0.125	0.902
rMFG	0.75 ± 0.29	0.77 ± 0.27	-0.733	0.471
rIPL	0.93 ± 0.63	0.97 ± 0.89	-0.751	0.461

mPerAF, mean percent amplitude of fluctuation; pre-rTMS, before rTMS session; post-rTMS, after rTMS session; dACC, dorsal anterior cingulate cortex; rMFG, right middle frontal gyrus; rIPL, right inferior parietal lobule; rMFG-target, rMFG single-target condition; rIPL-target, rIPL single-target condition; Double-targets, double-targets condition; *$P < 0.05$ uncorrected.

Discussion

The current study aimed to investigate two main issues: 1) whether the FC strength between the stimulation targets (rMFG- and rIPL-target) and the dACC could predict the local activity change in the dACC; and 2) whether MTF-rTMS could exert a focused effect on the dACC. The results revealed that rMFG-target stimulation significantly reduced local activity in the dACC. Furthermore, the strength of the dACC-rMFG FC was negatively correlated with the local activity change in the dACC. However, no significant difference was found among the four rTMS conditions (rMFG-target, rIPL-target, Double-targets, and Sham) in either the local activity change or FC change.

Direct Evidence of the rTMS Modulation Effect on Local Activity in a Deep/Remote Region

A line of RS-fMRI studies reported rTMS modulation effects on local spontaneous activity in deep or remote regions (Xue et al. 2017; Grohn et al. 2019; Guo et al. 2019; Ruan et al. 2019; Wang et al. 2020; Yin et al. 2020; Zheng et al. 2020; Yuan et al. 2021). For example, our recent study found that, compared with low-frequency rTMS, high-frequency rTMS over the primary motor cortex increased the local activity in the right cerebellum (Wang et al. 2020). However, none of these studies were FC-guided. Thus, although local activity in remote regions is indeed modulated by rTMS, it is unclear whether this modulation effect is transmitted via the FC from the stimulation target to the

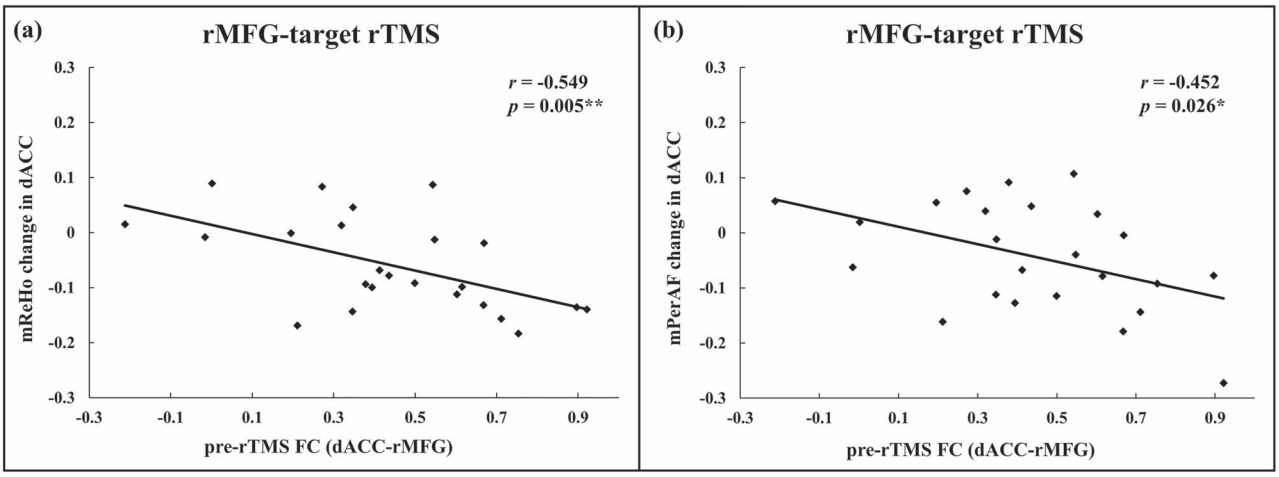

Figure 6. Correlation between pre-rTMS FC of dACC-rMFG and local activity changes of the dACC after stimulated the rMFG-target. (a) The pre-rTMS FC of dACC-rMFG in the rMFG-target condition significantly negative correlated with the mReHo change of the dACC. (b) The pre-rTMS FC of dACC-rMFG in the rMFG-target condition showed a negative trend with the mPerAF change of the dACC. mReHo, mean regional homogeneity; mPerAF, mean percent amplitude of fluctuation; FC, functional connectivity; dACC, dorsal anterior cingulate cortex; rMFG, right middle frontal gyrus; rMFG-target, rMFG single-target condition; *$P < 0.05$ uncorrected; **, still significant after Bonferroni correction of 0.05/6 = 0.008.

effective region. In addition, although some rTMS studies used RS-fMRI FC to guide precise stimulation targeting, none of these FC-guided TMS studies measured local activity in a remote brain region that was functionally connected to the superficial stimulation target (Wang et al. 2014; Wang and Voss 2015; Freedberg et al. 2019; Hendrikse et al. 2020).

In the current study, we found that the rMFG-target stimulation significantly reduced the local activity in the effective region (i.e., dACC). However, it should be noted that the significant local activity difference (i.e., post-rTMS versus pre-rTMS) in the effective region cannot exclude the possibility of a sequential effect. Hence, we explored this issue, and found that stronger dACC-rMFG FC strength before rMFG-target stimulation was associated with a greater decrease in local activity in the dACC (Fig. 6). The combined evidence indicates that FC-guided TMS applied to a superficial cortical target was able to modulate local activity in a remote effective region that is functionally connected to the superficial stimulation target.

The current results were ROI-based and hypothesis-driven. However, the stimulation target inevitably has more than one connected brain region. Thus, we performed additional voxel-wise group-level paired *t*-test (post-rTMS vs. pre-rTMS) (See more details in SM3 in Supplementary Material). The results revealed significantly increased local activity (mReHo) only in the middle temporal gyrus of the rMFG-target rTMS (Gaussian random field correction voxel-level $P < 0.001$, cluster $P < 0.05$) (Fig. S4). No significant difference was found in other pair-wise comparisons. Furthermore, we extracted the mean time-series of the cluster (52 voxels, middle temporal gyrus) and performed FC with the rMFG target ROI, and then performed correlation between FC strength and mReHo change. The correlation was not significant ($r = 0.053$, $P = 0.805$), suggesting that the FC strength of the rMFG-target and other brain regions did not predict local activity changes, except in the dACC. This finding warrants further investigation in future studies.

MTF-rTMS in dACC

Each seed region has widespread FC within the whole brain, including multiple superficial cortical areas (Eldaief et al. 2011; Tao et al. 2016; Lei et al. 2017; Zuo et al. 2017; Chen et al. 2018; Long et al. 2018; Facer-Childs et al. 2019). However, no previous FC-guided rTMS studies have used multiple stimulation targets via their own FC to focus the stimulation effects on the same effective region. It should be noted that although a few multi-target rTMS studies have been reported (Hendrikse et al. 2020; Mielacher et al. 2020), these studies involved stimulation of different effective regions. In the current study, we proposed the MTF-rTMS hypothesis. We adopted the individualized peak activation voxel in the dACC as the effective region, then defined two superficial cortical stimulation targets (the rMFG and rIPL) which showed strong FC with the effective region. No significant difference was found in the local activity change (i.e., post-rTMS minus pre-rTMS) in the dACC among the four stimulation conditions. Thus, we additionally performed an exploratory whole-brain voxel-wise one-way ANOVA, but no results survived the multiple comparison correction (Gaussian random field correction, voxel-level $P < 0.001$, cluster $P < 0.05$).

There are several possible reasons that the current findings failed to support the MTF-rTMS hypothesis: 1) We speculated that the FC strength between the dACC and rIPL would be weaker than that of dACC-rMFG. Therefore, we performed a paired *t*-test to compare the FC strength of the dACC-rMFG FC with that of the dACC-rIPL FC. The results revealed that dACC-rMFG FC was significantly higher than dACC-rIPL FC ($t = 3.54$, $P = 0.002$) (see Supplementary Material SM4; Fig. S5). This finding suggests that the failure of the results to support the MTF-rTMS hypothesis could be partially attributed to the weak FC strength of dACC-rIPL. 2) The anatomical distance between the effective region and the stimulation target may also be a factor. The distance from the dACC to the rMFG stimulation target was closer than that to rIPL. 3) There is large inter-individual variability in the location of task fMRI activation (i.e., the effective region). Inter-individual variability plays critical roles in response to the TMS (Lopez-Alonso et al. 2014; Beynel et al. 2020). Thus, we were trying to reduce the inter-individual variability by using a relatively simple cognitive task and a dACC mask. It has been proposed that the individual task fMRI activation (Wang et al. 2020) and patient-specific RS-fMRI FC (Cash et al. 2020) might be helpful for rTMS treatment. However, the extent to which exact

inter-individual variability influences rTMS effects is largely unknown and requires further investigation.

Test–Retest Reliability of Pre-rTMS FC

The reliability of FC is an important consideration. A previous study reported that the test–retest reliability of FC increases with longer acquisition time, and a minimum of 15 min of acquisition time is required to obtain moderate reliability (Mueller et al. 2015). The current study involved only 8 min of scanning. We calculated the test–retest reliability of pre-rTMS FC and found that the intra-class correlation (ICC) coefficients of the four visits were 0.392 and 0.428 for dACC-rMFG FC and dACC-rIPL FC, respectively (see Supplementary Material SM5).

Limitations

Several potential limitations of the current study should be considered. First, because the sample size was relatively small, it would be helpful to replicate the results in a larger scale study. Second, we did not measure behavioral performance. The current findings would be more robust if the local activity change of the dACC is accompanied by behavioral performance enhancement. Third, more functional imaging modalities should be used in future studies to investigate the modulation effects of MTF-rTMS more thoroughly, such as arterial spin labeling for detecting cerebral blood flow (CBF) and post-rTMS task MRI for detecting activation changes. Fourth, we positioned the coil 45° toward the contralateral forehead throughout the entire rTMS session. As suggested in a previous study, an individually optimized coil position and orientation based on the individual gyral crown would produce maximal electric fields (Weise et al. 2019). Fifth, we found that stronger dACC-rMFG FC strength before rMFG-target stimulation was associated with a greater decrease in local activity in the dACC. Because scanning before rTMS on each day is not clinically feasible, we calculated the correlation between the FC strength on Visit 1 (for defining targets) and the local activity change in the effective region in each of the four conditions. However, no significant correlation was found (see Supplementary Material SM6, Tables S2 and S3). A better predictor should be investigated in future studies. Sixth, the relatively large variation in spatial location of dACC activation and the weaker activation in some participants may have increased inter-subject variability and hence reduced the consistency of the results.

Conclusion

The present study revealed that the rMFG-target stimulation significantly decreased local activity in the dACC. We further found that a stronger dACC-rMFG FC could predict a larger modulation effect on the local activity in the dACC. The current study failed to validate the MTF-rTMS hypothesis. This finding was likely to have been caused by weak dACC-rIPL FC. Future studies with optimized parameters (e.g., stronger FC to guide the stimulation target) are needed to test the MTF-rTMS hypothesis more comprehensively.

Author Contributions

ZF searched the literature, recruited the subjects, collected the data, performed the data analysis, and wrote the manuscript. XD, NZ, YJ, and HW recruited the subjects and collected the data. NZ, JY, and YH assisted with the data analysis. TK and JJ revised the article. JW and YZ generated the research concept, contributed to the experimental design, and revised the article.

Supplementary Material

Supplementary material can be found at *Cerebral Cortex* online.

Data availability statement

The datasets of this article are not readily available because the raw data supporting the conclusions of this article will be made available by the authors upon request. Requests to access the datasets should be directed to the corresponding author. Human data will become available following the CCBD's regulations.

Funding

This research was supported by the National Natural Science Foundation of China (Nos 81701776, 31471084, 82071537, and 81520108016), Key Medical Discipline of Hangzhou, and Key Realm R&D Program of Guangdong Province (2019B030335001).

Notes

Conflict of Interests. The authors declare that they have no conflicts of interest.

References

Ahdab R, Ayache SS, Brugieres P, Goujon C, Lefaucheur JP. 2010. Comparison of "standard" and "navigated" procedures of TMS coil positioning over motor, premotor and prefrontal targets in patients with chronic pain and depression. *Neurophysiol Clin*. 40:27–36.

Beynel L, Powers JP, Appelbaum LG. 2020. Effects of repetitive transcranial magnetic stimulation on resting-state connectivity: a systematic review. *Neuroimage*. 211:116596.

Bush G. 2011. Cingulate, frontal, and parietal cortical dysfunction in attention-deficit/hyperactivity disorder. *Biol Psychiatry*. 69:1160–1167.

Bush G, Luu P, Posner MI. 2000. Cognitive and emotional influences in anterior cingulate cortex. *Trends Cogn Sci*. 4:215–222.

Cash RFH, Weigand A, Zalesky A, Siddiqi SH, Downar J, Fitzgerald PB, Fox MD. 2020. Using brain imaging to improve spatial targeting of transcranial magnetic stimulation for depression. *Biol Psychiatry*. S0006-3223(20):31668–1. https://doi.org/10.1016/j.biopsych.2020.05.033.

Cash RFH, Zalesky A, Thomson RH, Tian Y, Cocchi L, Fitzgerald PB. 2019. Subgenual functional connectivity predicts antidepressant treatment response to transcranial magnetic stimulation: independent validation and evaluation of personalization. *Biol Psychiatry*. 86:e5–e7.

Chen L, Wang Y, Niu C, Zhong S, Hu H, Chen P, Zhang S, Chen G, Deng F, Lai S, *et al*. 2018. Common and distinct abnormal frontal-limbic system structural and functional patterns in patients with major depression and bipolar disorder. *Neuroimage Clin*. 20:42–50.

Cole EJ, Stimpson KH, Bentzley BS, Gulser M, Cherian K, Tischler C, Nejad R, Pankow H, Choi E, Aaron H, *et al*. 2020. Stanford accelerated intelligent Neuromodulation therapy for treatment-resistant depression. *Am J Psychiatry*. 177:716–726.

Drevets WC, Savitz J, Trimble M. 2008. The subgenual anterior cingulate cortex in mood disorders. *CNS Spectr*. 13:663–681.

Eldaief MC, Halko MA, Buckner RL, Pascual-Leone A. 2011. Transcranial magnetic stimulation modulates the brain's intrinsic activity in a frequency-dependent manner. *Proc Natl Acad Sci U S A*. 108:21229–21234.

Eriksen BA, Eriksen CW. 1974. Effects of noise letters upon the identification of a target letter in a nonsearch task. *Percept Psychophys*. 16:143–149.

Facer-Childs ER, Campos BM, Middleton B, Skene DJ, Bagshaw AP. 2019. Circadian phenotype impacts the brain's resting-state functional connectivity, attentional performance, and sleepiness. *Sleep*. 42(5):zsz033. https://doi.org/10.1093/sleep/zsz033.

Fox MD, Buckner RL, White MP, Greicius MD, Pascual-Leone A. 2012. Efficacy of transcranial magnetic stimulation targets for depression is related to intrinsic functional connectivity with the subgenual cingulate. *Biol Psychiatry*. 72:595–603.

Freedberg M, Reeves JA, Toader AC, Hermiller MS, Voss JL, Wassermann EM. 2019. Persistent enhancement of hippocampal network connectivity by parietal rTMS is reproducible. *eNeuro*. 6(5):ENEURO.0129-19.2019. https://doi.org/10.1523/ENEURO.0129-19.2019.

Grohn H, Gillick BT, Tkac I, Bednarik P, Mascali D, Deelchand DK, Michaeli S, Meekins GD, Leffler-McCabe MJ, MacKinnon CD, *et al*. 2019. Influence of repetitive transcranial magnetic stimulation on human neurochemistry and functional connectivity: a pilot MRI/MRS study at 7 T. *Front Neurosci*. 13:1260.

Guo Z, Jiang Z, Jiang B, McClure MA, Mu Q. 2019. High-frequency repetitive transcranial magnetic stimulation could improve impaired working memory induced by sleep deprivation. *Neural Plast*. 2019:7030286.

Hendrikse J, Coxon JP, Thompson S, Suo C, Fornito A, Yucel M, Rogasch NC. 2020. Multi-day rTMS exerts site-specific effects on functional connectivity but does not influence associative memory performance. *Cortex*. 132:423–440.

Herbsman T, Avery D, Ramsey D, Holtzheimer P, Wadjik C, Hardaway F, Haynor D, George MS, Nahas Z. 2009. More lateral and anterior prefrontal coil location is associated with better repetitive transcranial magnetic stimulation antidepressant response. *Biol Psychiatry*. 66:509–515.

Herwig U, Padberg F, Unger J, Spitzer M, Schonfeldt-Lecuona C. 2001. Transcranial magnetic stimulation in therapy studies: examination of the reliability of "standard" coil positioning by neuronavigation. *Biol Psychiatry*. 50:58–61.

Jia X-Z, Wang J, Sun H-Y, Zhang H, Liao W, Wang Z, Song X, Zang Y-F. 2019. RESTplus: an improved toolkit for resting-state functional magnetic resonance imaging data processing. *Science Bulletin*. 64(14):953–954. https://doi.org/10.1016/j.scib.2019.05.008.

Jia XZ, Sun JW, Ji GJ, Liao W, Lv YT, Wang J, Wang Z, Zhang H, Liu DQ, Zang YF. 2020. Percent amplitude of fluctuation: a simple measure for resting-state fMRI signal at single voxel level. *PLoS One*. 15(1):e0227021. https://doi.org/10.1371/&break;journal.pone.0227021.

Jing Y, Zhao N, Deng X-P, Feng Z-J, Huang G-F, Meng M, Zang Y-F, Wang J. 2020. Pregenual or subgenual anterior cingulate cortex as potential effective region for brain stimulation of depression. *Brain Behav*. 10(4):e01591. https://doi.org/10.1002/brb3.1591.

Lee YJ, Koo BH, Seo WS, Kim HG, Kim JY, Cheon EJ. 2017. Repetitive transcranial magnetic stimulation of the supplementary motor area in treatment-resistant obsessive-compulsive disorder: an open-label pilot study. *J Clin Neurosci*. 44:264–268.

Lei D, Du M, Wu M, Chen T, Huang X, Du X, Bi F, Kemp GJ, Gong Q. 2015. Functional MRI reveals different response inhibition between adults and children with ADHD. *Neuropsychology*. 29:874–881.

Lei X, Zhong M, Liu Y, Jin X, Zhou Q, Xi C, Tan C, Zhu X, Yao S, Yi J. 2017. A resting-state fMRI study in borderline personality disorder combining amplitude of low frequency fluctuation, regional homogeneity and seed based functional connectivity. *J Affect Disord*. 218:299–305.

Li CT, Chen MH, Juan CH, Huang HH, Chen LF, Hsieh JC, Tu PC, Bai YM, Tsai SJ, Lee YC, *et al*. 2014. Efficacy of prefrontal theta-burst stimulation in refractory depression: a randomized sham-controlled study. *Brain*. 137:2088–2098.

Long X, Liu F, Huang N, Liu N, Zhang J, Chen J, Qi A, Guan X, Lu Z. 2018. Brain regional homogeneity and function connectivity in attenuated psychosis syndrome -based on a resting state fMRI study. *BMC Psychiatry*. 18:383.

Lopez-Alonso V, Cheeran B, Rio-Rodriguez D, Fernandez-Del-Olmo M. 2014. Inter-individual variability in response to non-invasive brain stimulation paradigms. *Brain Stimul*. 7:372–380.

Mielacher C, Schultz J, Kiebs M, Dellert T, Metzner A, Graute L, Högenauer H, Maier W, Lamm C, Hurlemann R. 2020. Individualized theta-burst stimulation modulates hippocampal activity and connectivity in patients with major depressive disorder. *Personalized Medicine in Psychiatry*. 23:100066.

Morecraft R, Tanji J. 2009. Cingulofrontal interactions and the cingulate motor areas. In: Vogt B, editor. *Cingulate Neurobiology and Disease*. New York: Oxford University Press, pp. 113–144.

Mueller S, Wang D, Fox MD, Pan R, Lu J, Li K, Sun W, Buckner RL, Liu H. 2015. Reliability correction for functional connectivity: theory and implementation. *Hum Brain Mapp*. 36:4664–4680.

Norman LJ, Carlisi C, Lukito S, Hart H, Mataix-Cols D, Radua J, Rubia K. 2016. Structural and functional brain abnormalities in attention-deficit/hyperactivity disorder and obsessive-compulsive disorder: a comparative meta-analysis. *JAMA Psychiat*. 73:815–825.

Padmanabhan JL, Cooke D, Joutsa J, Siddiqi SH, Ferguson M, Darby RR, Soussand L, Horn A, Kim NY, Voss JL, *et al*. 2019. A human depression circuit derived from focal brain lesions. *Biol Psychiatry*. 86:749–758.

Pascual-Leone A, Rubio B, Pallardo F, Catala MD. 1996. Rapid-rate transcranial magnetic stimulation of left dorsolateral prefrontal cortex in drug-resistant depression. *Lancet*. 348:233–237.

Rolls E. 2009. The anterior and midcingulate cortices and reward. In: Vogt B, editor. *Cingulate Neurobiology and Disease*. New York: Oxford University Press, pp. 191–206.

Rossini PM, Burke D, Chen R, Cohen LG, Daskalakis Z, Di Iorio R, Di Lazzaro V, Ferreri F, Fitzgerald PB, George MS, *et al*. 2015. Non-invasive electrical and magnetic stimulation of the brain, spinal cord, roots and peripheral nerves: basic principles and procedures for routine clinical and research application. An updated report from an I.F.C.N. committee. *Clin Neurophysiol*. 126:1071–1107.

Ruan X, Zhang G, Xu G, Gao C, Liu L, Liu Y, Jiang L, Zhang S, Chen X, Jiang X, *et al*. 2019. The after-effects of theta burst stimulation over the cortex of the suprahyoid muscle on regional homogeneity in healthy subjects. *Front Behav Neurosci*. 13:35.

Shehata HS, Esmail EH, Abdelalim A, El-Jaafary S, Elmazny A, Sabbah A, Shalaby NM. 2016. Repetitive transcranial magnetic stimulation versus botulinum toxin injection in chronic

migraine prophylaxis: a pilot randomized trial. *J Pain Res*. 9:771–777.

Siddiqi SH, Trapp NT, Hacker CD, Laumann TO, Kandala S, Hong X, Trillo L, Shahim P, Leuthardt EC, Carter AR, *et al*. 2019. Repetitive transcranial magnetic stimulation with resting-state network targeting for treatment-resistant depression in traumatic brain injury: a randomized, controlled, double-blinded pilot study. *J Neurotrauma*. 36:1361–1374.

Tao J, Liu J, Egorova N, Chen X, Sun S, Xue X, Huang J, Zheng G, Wang Q, Chen L, *et al*. 2016. Increased hippocampus-medial prefrontal cortex resting-state functional connectivity and memory function after tai chi Chuan practice in elder adults. *Front Aging Neurosci*. 8:25.

Tzourio-Mazoyer N, Landeau B, Papathanassiou D, Crivello F, Etard O, Delcroix N, Mazoyer B, Joliot M. 2002. Automated anatomical labeling of activations in SPM using a macroscopic anatomical parcellation of the MNI MRI single-subject brain. *Neuroimage*. 15:273–289.

Wang J, Deng XP, Wu YY, Li XL, Feng ZJ, Wang HX, Jing Y, Zhao N, Zang YF, Zhang J. 2020. High-frequency rTMS of the motor cortex modulates cerebellar and widespread activity as revealed by SVM. *Front Neurosci*. 14:186.

Wang J, Liu DQ, Zhang H, Zhu WX, Dong ZY, Zang YF. 2013. Asymmetry of the dorsal anterior cingulate cortex: evidences from multiple modalities of MRI. *Neuroinformatics*. 11: 149–157.

Wang J, Yang N, Liao W, Zhang H, Yan CG, Zang YF, Zuo XN. 2015. Dorsal anterior cingulate cortex in typically developing children: laterality analysis. *Dev Cogn Neurosci*. 15: 117–129.

Wang JX, Rogers LM, Gross EZ, Ryals AJ, Dokucu ME, Brandstatt KL, Hermiller MS, Voss JL. 2014. Targeted enhancement of cortical-hippocampal brain networks and associative memory. *Science*. 345:1054–1057.

Wang JX, Voss JL. 2015. Long-lasting enhancements of memory and hippocampal-cortical functional connectivity following multiple-day targeted noninvasive stimulation. *Hippocampus*. 25:877–883.

Weigand A, Horn A, Caballero R, Cooke D, Stern AP, Taylor SF, Press D, Pascual-Leone A, Fox MD. 2018. Prospective validation that Subgenual connectivity predicts antidepressant efficacy of transcranial magnetic stimulation sites. *Biol Psychiatry*. 84:28–37.

Weise K, Numssen O, Thielscher A, Hartwigsen G, Knosche TR. 2019. A novel approach to localize cortical TMS effects. *Neuroimage*. 209:116486.

Williams NR, Sudheimer KD, Bentzley BS, Pannu J, Stimpson KH, Duvio D, Cherian K, Hawkins J, Scherrer KH, Vyssoki B, *et al*. 2018. High-dose spaced theta-burst TMS as a rapid-acting antidepressant in highly refractory depression. *Brain*. 141(3):e18. https://doi.org/10.1093/brain/awx379.

Xue SW, Guo Y, Peng W, Zhang J, Chang D, Zang YF, Wang Z. 2017. Increased low-frequency resting-state brain activity by high-frequency repetitive TMS on the left dorsolateral prefrontal cortex. *Front Psychol*. 8:2266.

Yan H, Zuo XN, Wang D, Wang J, Zhu C, Milham MP, Zhang D, Zang Y. 2009. Hemispheric asymmetry in cognitive division of anterior cingulate cortex: a resting-state functional connectivity study. *Neuroimage*. 47:1579–1589.

Yin M, Liu Y, Zhang L, Zheng H, Peng L, Ai Y, Luo J, Hu X. 2020. Effects of rTMS treatment on cognitive impairment and resting-state brain activity in stroke patients: a randomized clinical trial. *Front Neural Circuits*. 14:563777.

Yuan LQ, Zeng Q, Wang D, Wen XY, Shi Y, Zhu F, Chen SJ, Huang GZ. 2021. Neuroimaging mechanisms of high-frequency repetitive transcranial magnetic stimulation for treatment of amnestic mild cognitive impairment: a double-blind randomized sham-controlled trial. *Neural Regen Res*. 16:707–713.

Zang Y, Jiang T, Lu Y, He Y, Tian L. 2004. Regional homogeneity approach to fMRI data analysis. *Neuroimage*. 22:394–400.

Zang YF, He Y, Zhu CZ, Cao QJ, Sui MQ, Liang M, Tian LX, Jiang TZ, Wang YF. 2007. Altered baseline brain activity in children with ADHD revealed by resting-state functional MRI. *Brain Dev*. 29:83–91.

Zhao N, Yuan LX, Jia XZ, Zhou XF, Deng XP, He HJ, Zhong J, Wang J, Zang YF. 2018. Intra- and inter-scanner reliability of voxel-wise whole-brain analytic metrics for resting state fMRI. *Front Neuroinform*. 12:54.

Zheng A, Yu R, Du W, Liu H, Zhang Z, Xu Z, Xiang Y, Du L. 2020. Two-week rTMS-induced neuroimaging changes measured with fMRI in depression. *J Affect Disord*. 270:15–21.

Zuo L, Wang S, Yuan J, Gu H, Zhou Y, Jiang T. 2017. Altered intra- and interregional synchronization in the absence of the corpus callosum: a resting-state fMRI study. *Neurol Sci*. 38:1279–1286.